J. Electroanal. Chem., 148 (1983) 249–270
Elsevier Sequoia S.A., Lausanne – Printed in The Netherlands

A CONFORMATIONAL ANALYSIS OF PROPYLENE CARBONATE MOLECULES ADSORBED AT THE MERCURY ELECTRODE

R. BRASSEUR and H.D. HURWITZ

Université Libre de Bruxelles, Service de Chimie Analytique et Minérale, C.P. 160, 50 av. F.D. Roosevelt, 1050 Bruxelles (Belgium)

(Received 23rd July 1982)

ABSTRACT

A programme has been conceived which applies to conformation analysis of propylene carbonate molecules adsorbed at the Hg electrode. Several molecular orientations are selected in order to fix the atoms, bearing point charges, in the configuration space. Calculations are performed with semi-empirical functions representing the energy terms of molecular clusters. Atom–atom and point-charge–point-charge interactions are used to determine the van der Waals interaction between adsorbed molecules. Dispersion components of the atom–metal phase interaction and self-image interactions of point charges yield the metal phase-adsorbed molecule van der Waals interaction. The effects of the internal molecular degrees of freedom and of the external electric field upon the molecular point dipole have been taken into account.

The ensemble distribution function, computed within the limits of doublet interaction leads to the evaluation of the average dipole moment and the inner-layer capacity. This theoretical value is compared to the experimental inner-layer capacitance measured in the propylene carbonate solvent–Hg electrode system.

INTRODUCTION

Hydrogen bonds and molecular internal degrees of freedom should contribute markedly to the overall stability of water adsorbed at the polarizable electrode interface. These physico-chemical factors make the stereochemical translation of water adsorption into simple molecular models difficult. For this reason, we might expect that the adsorption of some aprotic solvents could be more easily handled with such molecular models. An even more drastic simplification of the model may be achieved in the case of propylene carbonate or ethylene carbonate molecules, due to the relative rigidity of the heteronuclear ring. Such systems have been investigated at the Hg interface [1–6] and have been explained theoretically according to the hypothesis that there are two [7–9] or three [10,11] possible configurations of solvent monomers, or both monomers and clusters [12]. The molecules are considered to be hard spheres containing a point dipole at their centre, the dipole vector being oriented in the direction of the electrode field (up position) or opposite (down position) in the two-state model. In addition, the three-state model makes allowance for a position parallel to the electrode surface and consequently provides a much

0022-0728/83/$03.00

better agreement with the experimental results. The calculations in the three-state model yield a principal extremum (a maximum or minimum) for the inner-layer differential capacity curves and allow the experimental data to be represented by a function with only two adjustable parameters, the average or isotropic polarizability and the nearest-neighbour distance respectively. Yet, the residual energies corresponding to the specific interaction at each orientation of the molecules with the metal are estimated from the values of the electrode charge density and the values of the corresponding inner-layer capacity at its extremum. These conditions force the theoretical and experimental curves to coincide at this point.

The three-state model predicts that the capacity curves will be symmetrical with respect to this principal extremum, a result which is not observed experimentally. More recently a multistate model for the solvent structure and dielectric properties at the interface was suggested [13]. Such a continuous spectrum of orientations of the hard-sphere point dipole molecules in the inner layer has led to asymmetric inner-layer capacity curves with respect to the charge. However, this multistate version of the theory overlooks the fact that some configurations of the solvent dipoles at the surface are not possible because of steric properties of the molecules. Furthermore, it is obvious that neither the three-state nor the multistate model make use of correct van der Waals forces and both fail to bring out consistent electrostatic interactions between close-packed molecules. The fact that no provision is made in the models for mutual interaction of molecules with parallel-ordered dipoles with respect to the surface confirms the weakness of these treatments.

It thus seems necessary to elaborate a theory of adsorption at the electrode on the basis of a molecular model which is meaningful in both the steric and electronic configurational levels. Having thus selected a number of most probable orientations, we may calculate the energies of pairs or of larger aggregations of molecules and predict their average conformation by minimizing the lattice energy. The present work aims at being a preliminary attempt in this direction. We have undertaken a systematic conformational analysis of adsorbed monolayers which are built up with simple rigid molecules having only a few internal rotational degrees of freedom. We have used Coulomb's law for the interaction of all atoms bearing a point charge as resulting from the electronic density mapping of the molecules. A semi-empirical atom–atom potential energy relationship has been introduced for the intermolecular and mercury-adsorbed molecule van der Waals forces.

With a view to testing the computational method and the empirical construction of the adsorbed molecular system, the present treatment has been confined within the following limits.

First, an analysis has been performed of only the most stable conformations of clusters of similarly oriented molecules. Second, interaction energy terms of molecular doublets only have been taken in account in the analysis of monolayers constituted of differently oriented molecules. A more extensive study of large clusters of differently oriented molecules will be subject of a forthcoming publication.

The conformational analysis here is applied to the propylene carbonate–mercury

electrode interphase. In this case, our electrocapillary measurements as a function of temperature have furnished the values of the differential capacities, as well as some indication concerning the molecular orientation at the surface [6].

DEFINITION OF ENERGY TERMS

In the isolated propylene carbonate (PC) molecule, conformational changes occur solely through rotation of the methyl group around the C–C bond. The internal molecular potential energy of torsion around this bond is taken into account by means of the relation [14]

$$E_p^{\mathrm{Tor}} = \tfrac{1}{2} E_0^{\mathrm{Tor}} (1 + \cos 3\theta_p) \tag{1}$$

where $E_0^{\mathrm{Tor}} = 11.7$ kJ mol^{-1} is the energy in the eclipsed conformation ($\theta_p = 0$). This value corresponds to the energy barrier maximum associated with the transition between two staggered conformations.

Given a molecular orientation relative to the surface, the atoms of the PC molecules are fixed in the conformational space by taking into account the values of bond angles and lengths shown in Fig. 1. The complete set of spatial coordinates of one molecule p corresponding to one orientation is defined as $(\alpha)_p$. In this investigation, five orientation, labelled A, B, C, D and E have been considered. We also define by α or β an element of the set of orientations (A, B, C, D, E). The orientations considered here are depicted in Fig. 2 and are as follows:

Orientation A. Vertically adsorbed molecules with their C=O function pointing towards the metal, the C=O bond axis being in the direction of the Z-axis perpendicular to the surface placed in the X–Y plane.

Orientation B. Molecules adsorbed with the C=O function pointing towards the metal, the C=O bond axis and the plane of the heterocycle forming an angle of 45° with the surface.

Orientation C. Molecules lying nearly flat on the surface *.

Orientation D. Molecules adsorbed with the C=O function pointing towards the metal, the plane of the heterocycle being perpendicular to the surface plane and the oxygen of the ring at the α position of the methyl-substituted carbon being in contact with the metal surface. This corresponds to an angle of about 30° between the surface plane and the O=C bond.

* Because of the difference of van der Waals radius of the oxygen atom (0.14 nm) and C–H groups (0.19 nm), an angle of inclination between the surface plane and the heterocycle of about 8° is observed, as indicated later.

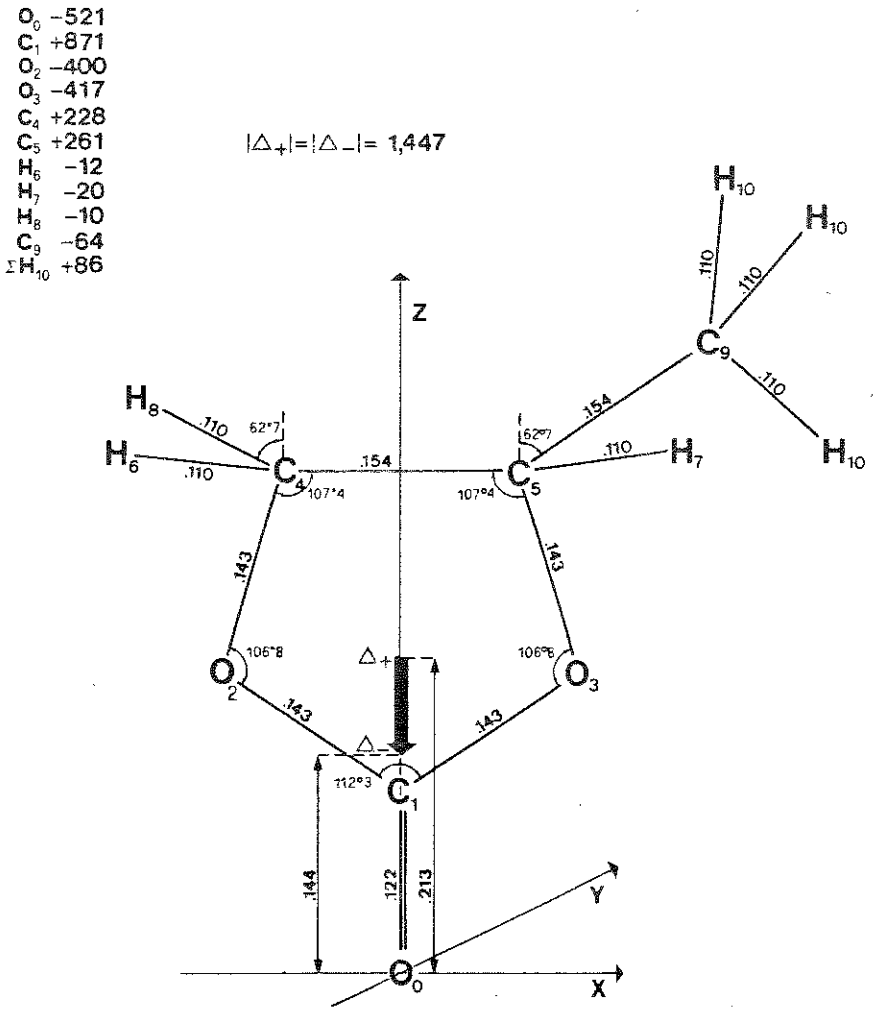

Fig. 1. The geometry and point-charge (in 10^{-3} electron charge unit) representation used in the calculation of propylene carbonate molecules with indication of the localization of the dipole moment projection along axis Z in orientation A (see text).

Orientation E. Vertically adsorbed molecules with their C=O function pointing towards the solution, the C=O axis being in the direction Z.

The zero energy level is considered to be the energy of the isolated molecule with the $\rangle$CH–CH$_3$ group in staggered conformation.

The conformational energy of a given set of N rigid molecules fixed in the conformational space is characterized by the complete coordinate set $\{\alpha\}\equiv\{\alpha\}_1$ $\{\alpha\}_2 \ldots .\{\alpha\}_p .. \{\alpha\}_N$ and has been computed as a sum of the following terms:

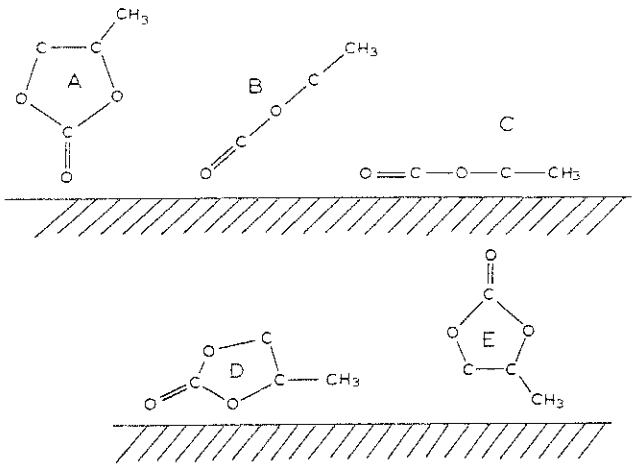

Fig. 2. Molecular orientations used in the calculation.

(1) The London–van der Waals energy of interaction between all pairs of non-mutually bonded atoms. Buckingham's pairwise atom–atom interaction functions have been used [15].

$$E_{\{\alpha\}}^{(N)\text{V.d.W.}} = \sum_{i,j} \left(E_{i,j}\right)_{\{\alpha\}} = \sum_{i,j} \left[A_{i,j} \exp\left(-B_{i,j} r_{ij}\right) - C_{i,j} r_{ij}^{-6}\right] \tag{2}$$

where $j = 1, 2\ldots$ are the non-bonded atoms, r_{ij} their distances from each other and $A_{i,j}$, $B_{i,j}$, $C_{i,j}$ are coefficients assigned to atom pairs. The values of these coefficients have been reported by Liquori and Giglio [16,17]. Like other quantum mechanical results [18], these values emerge in part as the solution of the Schrödinger equation and in part as heuristic variables. They have been applied with success to conformational analysis of molecular crystals, proteins and polypeptides [19–21]. The semi-empirical constants used in this work are given in Table 1. In order to compensate the decrease of the function represented by eqn. (2) at small r_{ij}, we have imposed an arbitrary cut-off value of $E_{i,j}^{\text{V.d.W.}} = 418$ kJ mol^{-1} at $r_{ij} < 0.1$ nm.

(2) The generalized Keesom–van der Waals interaction or electrostatic interaction between atomic point charges.

At distances comparable to the molecular size, it becomes undubitably less correct to deal with point dipoles rather than with atomic point-charge distributions. The coulombic interaction energies corresponding to such distributions include all higher-order terms (quadrupoles, octopoles...) which are usually neglected. Formally, the energy can be written as follows:

$$E_{\{\alpha\}}^{(N)\text{cb}} = 139.2 \left(\sum_{i,j} \frac{e_i e_j}{r_{ij}} \right)_{\{\alpha\}} \text{(kJ mol}^{-1}\text{)} \tag{3}$$

TABLE 1

Semi-empirical constants used in this work

$i-j$	$10^3 A_{ij}$ / kJ mol^{-1}	B_{ij} / nm^{-1}	$10^6 C_{ij}$ / kJ nm^6 mol^{-1}
O–O	779.9	190.372	836.8
O–C	887.4	185.560	1020.9
O–methyl	1171.9	164.808	3209.5
O–H	117.7	180.581	415.1
C–C	991.6	180.749	1256.0
C–Methyl	1215.9	159.996	3916.2
C–H	131.3	175.770	506.7
Methyl–methyl	1146.0	139.285	12309.3
Methyl–H	171.9	155.017	1592.4
H–H	276.0	170.791	205.9

where e_i and e_j are expressed in electron charge units and r_{ij} in nm. The electron-density mapping of the PC molecule is given in Fig. 1 where each atom has been identified by means of an alphanumeric code. The values of the atomic point charges result from the application of the CNDO/2 method [22]. They agree well with the true value of $4.94D$ for the dipole moment.

(3) The potential energy of rotation of the methyl-substituted groups.

This rotation around the ethane-like C–C bond in a molecule p pertaining to the selected set $\{\alpha\}$ yields an energy given by eqn. (1). Thus, for N molecules, we have

$$E_{\{\alpha\}}^{(N)\mathrm{Tor}} = N_{\mathrm{Av}} \left(\sum_{p=1} E_p^{\mathrm{Tor}} \right)_{\{\alpha\}} \tag{4}$$

(4) The dispersion component of the energy of interaction between the metal and the adsorbed molecules.

Up to now this term has seldom been stated explicitly, although in the absence of covalent bonding, the London or dispersion component is the largest attractive contribution in virtually all cases of adsorption of neutral species. In the case of halide ion adsorption on Hg, Andersen and Bockris [23] introduced the London–van der Waals forces. In doing so, the assumption was implicitly made that the polarizability of mercury atoms and metallic mercury is the same. For our purposes, we preferred to work backwards, from macroscopic surface properties of the metal phase towards the molecular interaction parameters. As it turns out, the interaction energies may be deduced from the dispersion component of the surface tension of mercury [24] and from the semi-empirical constants C_{ii} recorded in Table 1 for different atoms i. Since the separation between the Hg and the molecule is of the same order of magnitude as the spacing between the atoms in the metal lattice, some discreteness of the metallic phase has been taken into account. The model and treatment are described in the Appendix. They yield the following expression for the attractive part of the potential energy:

$$E_{(\alpha)}^{(N)\mathrm{M.L.}} = \left(\sum_{i} \sum_{n=0}^{\infty} \frac{H_{i,\mathrm{Hg}}}{\left[Z_i + \left(r_{\mathrm{Hg}} + n d_{\mathrm{Hg}} \right) \right]^4} \right)_{(\alpha)} \tag{5}$$

with $r_{\mathrm{Hg}} = 0.189$ nm and $d_{\mathrm{Hg}} = \sqrt{3} \cdot (0.157)$ nm, where Z_i is the coordinate along Z of the atom i, and r_{Hg} and d_{Hg} the van der Waals radius and lattice plane spacing in a close-packing structure of mercury atoms. The definition of the constants $H_{i,\mathrm{Hg}}$ can be found in the Appendix and their values are recorded in Table 2. The resulting potential energy is shown as a function of distance in Fig. 3. The model of interaction also involves a potential energy of repulsion which sets in and rises vertically when the distance of approach Z_i equals the van der Waals radius of the atom in closest contact with the metal. A more realistic potential energy function would manifest a finite slope with an inverse 12th power dependence of Z_i. In the absence of reliable repulsion coefficients, such an inverse power law is not postulated in this treatment. The total potential energy function therefore displays a minimum as indicated in Fig. 3 which, for our computational purposes, describes sufficiently well the equilibrium position of the adsorbed species.

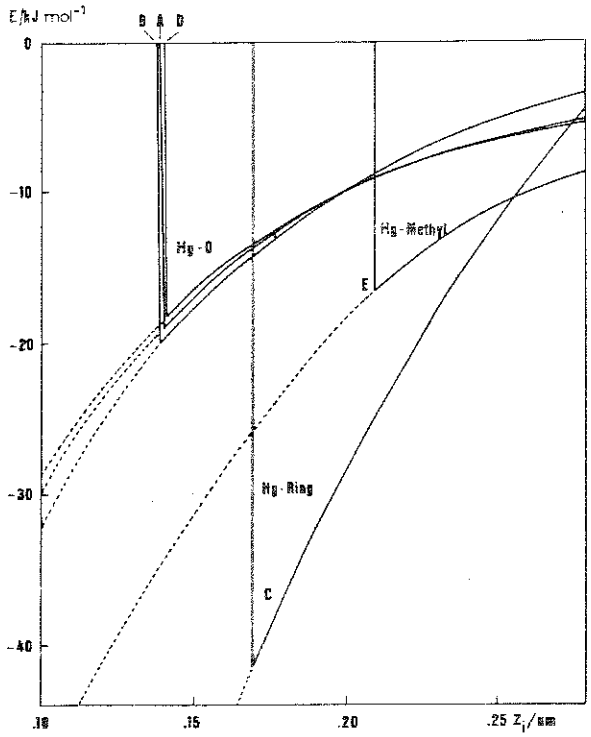

Fig. 3. Dispersion component of the potential energy of the adsorbed molecule–metal phase interaction vs. distance from the electrode surface.

TABLE 2

Values of $H_{i,Hg}$ for different atoms

i	H	C	O	Methyl
$10^4 H_{i,Hg}$/ kJ nm^4 mol^{-1}	188.25	485.80	508.35	1456.65

(5) The self-image interaction energy, of the point-charge distribution with the metal.

This term is in principle equivalent to the Debye component (permanent dipole–induced dipole interaction) of the van der Waals interaction energy of the adsorbed molecules with the metal. Similar to the method adopted in paragraph (2), we sum the self-image interaction energy corresponding to point-charge distributions belonging to the set of N molecules. According to paragraph (4), the surface envisaged as a perfectly electrical reflecting plane, is localized at a distance equal to the van der Waals radius of the atoms in contact with it. Thus one obtains

$$E_{\langle\alpha\rangle}^{(N)\mathrm{Im}} = \left(-\frac{139.2}{2} \sum_{i,j} \frac{e_i e_j}{\left[\left(Z_i + Z_j \right)^2 + X_{ij}^2 + Y_{ij}^2 \right]^{1/2}} \right)_{\langle\alpha\rangle} \quad (\mathrm{kJ\ mol^{-1}}) \tag{6}$$

where X_{ij}, Y_{ij} are the components of r_{ij} along the X- and Y-axis.

(6) The potential energy of the molecules in the external electric field.

The external field is created by a finite, uniform charge density q spread over the metal surface. The electric potential energy of the point-charge distribution in this field is calculated according to the relationship

$$E_{\langle\alpha\rangle}^{(N)\mathrm{Fld}} = N_{\mathrm{Av}} \left(\sum_{p=1}^{N} E_p^{\mathrm{Fld}} \right)_{\langle\alpha\rangle} = \frac{227.1}{\varepsilon_r} \cdot q \left(\sum_{p=1}^{N} (\mu_Z)_p \right)_{\langle\alpha\rangle} \quad (\mathrm{kJ\ mol^{-1}}) \tag{7}$$

where q is expressed in C m^{-2} and $(\mu_Z)_p$, the point-dipole moment projection along Z of molecule p, in Debye units. The dielectric constant ε_r, or distortional origin, is introduced in order to account for the influence of molecular polarizabilities. The terms considered in paragraphs (1) and (4) make allowance for some of the effects related to these polarizabilities. However, one still has to consider the contribution of the local electric field acting upon μ_p, produced by the induced dipole components of the surrounding molecules. Hence, the total local electric field becomes

$$\frac{q}{\varepsilon_0 \varepsilon_r} = \frac{q}{\varepsilon_0} + X_{\mathrm{pol}} \tag{8}$$

and

$$X_{\mathrm{pol}} = -\frac{1}{4\pi} \left\langle \frac{\alpha}{r^3} \right\rangle \left(\frac{q}{\varepsilon_0} + X_{\mathrm{pol}} \right) \tag{9}$$

where $\langle \alpha / r^3 \rangle$ represents a yet unknown function of the average polarizability of the

atomic groups and of the cube of their average distance r. We do not make this function further explicit here and will keep ε_r as an adjustable parameter of our treatment. One obtains from eqns. (8) and (9) that

$$4\pi(\varepsilon_r - 1) = \langle \alpha / r^3 \rangle \tag{10}$$

The total conformational energy of a set of N molecules adsorbed at the mercury electrode surface is now expressed as the sum of all terms defined above.

$$E_{\{\alpha\}}^{(N)} = E_{\{\alpha\}}^{(N)\text{V.d.W.}} + E_{\{\alpha\}}^{(N)\text{Cb}} + E_{\{\alpha\}}^{(N)\text{Tor}} + E_{\{\alpha\}}^{(N)\text{M.L.}} + E_{\{\alpha\}}^{(N)\text{Im}} + E_{\{\alpha\}}^{(N)\text{Fld}} \tag{11}$$

STRATEGY OF COMPUTATION

In this preliminary study, we wished to keep the number of selected conformations easily manageable. With this purpose in mind, we have adopted the following strategies.

Method 1

A set of 11 molecules belonging to the same class of orientations, either A, B, C, D or E is built up, step by step, by the addition of the Nth molecule to a previous set of $N-1$ molecules which is taken in its lowest conformational energy $E_{\{\alpha\}\min}^{(N-1)}$. The monolayer assemblage occurs by varying the following parameters:

(a) The translation of Nth molecule in the surface plane apart from the set of $N-1$ molecules.

(b) The rotation of the Nth molecule and of the set of $N-1$ molecules around their respective central axis in the Z-direction.

(c) The vertical displacement along the Z-axis of the Nth molecule with respect to the fixed set of $N-1$ molecules.

(d) The inclination of the Nth molecule with respect to the set of $N-1$ molecules. The $\rangle$C=O bond axis is inclined by angles comprised between $\pm 15°$ with respect to the direction of the axis corresponding to the initially selected orientation.

By changing these four conformational parameters, labelled respectively a, b, c, d, we have limited the computation to 2140 distinct molecular configurations per added molecule. This procedure yields:

(1) the atomic coordinates $\{\alpha\}$ in the conformational space corresponding to the deepest internal energy minimum $E_{\{\alpha\}\min}^{(N)}$ of a monolayer consisting of 11 molecules in a given orientation α;

(2) the average molecular projected area a_α on the metal surface.

Method 2

A conformational analysis has been performed on a pair of similarly oriented particles. The average pairwise energy brought about by varying the parameters considered in method 1 under (b), (c) and (d), has been computed at selected

intermolecular distances. According to our definition, we have

$$E^{(2)}_{\alpha\alpha} = \frac{\sum_{\{\alpha\}_1}\sum_{\{\alpha\}_2} E^{(2)}_{\{\alpha\}_1\{\alpha\}_2} \exp - \left(E^{(2)}_{\{\alpha\}_1\{\alpha\}_2}/RT\right)}{\sum_{\{\alpha\}_1}\sum_{\{\alpha\}_2} \exp - \left(E^{(2)}_{\{\alpha\}_1\{\alpha\}_2}/RT\right)} \tag{12}$$

$\alpha \in \{A, B, C, D, E\}$

where $E^{(2)}_{\{\alpha\}_1\{\alpha\}_2}$ represents the pairwise potential energy corresponding to one of the spatial localizations of molecules 1 and 2 as specified by the conformational parameters under (b), (c) and (d). The number of different configurations, which equals the number of elements of the set $\{\alpha\}_1 \cdot \{\alpha\}_2$ has been restricted to 144.000.

Method 3

A more detailed procedure has been performed on pairs of particles, each of the particles of the pair being selected in any of the A, B, C, D, and E orientations. This amounts to 15 different pairs $\alpha\beta$. While describing the whole conformational space by means of the four parameters specified in method 1 under (a), (b), (c) and (d), we have selected a number of distinct configurations of each couple or elements of $\{\alpha\}_1 \cdot \{\beta\}_2$ equal to 1,400.000. The ensemble average of the pairwise interaction energy has thus been performed, taking into account this number of arrangements, hence

$$E^{(2)}_{\alpha\beta} = \frac{\sum_{\{\alpha\}_1}\sum_{\{\beta\}_2} E^{(2)}_{\{\alpha\}_1\{\beta\}_2} \exp - \left(E^{(2)}_{\{\alpha\}_1\{\beta\}_2}/RT\right)}{\sum_{\{\alpha\}_1}\sum_{\{\beta\}_2} \exp - \left(E^{(2)}_{\{\alpha\}_1\{\beta\}_2}/RT\right)} \tag{13}$$

$\alpha, \beta \in \{A, B, C, D, E\}$

The evaluation of ensemble distribution function, characteristic of each orientation A, B, C, D and E, has been obtained from the expression

$$n_\alpha = \frac{\sum_{\alpha}(1 + \delta_{\alpha\beta}) \exp - \left(E^{(2)}_{\alpha\beta}/RT\right)}{2\sum_{\alpha}\sum_{\beta} \exp - \left(E^{(2)}_{\alpha\beta}/RT\right)} \tag{14}$$

where

$\delta_{\alpha\beta} = 1 \quad$ if $\alpha = \beta$

$= 0 \quad$ if $\alpha \neq \beta$

and

$\alpha, \beta \in \{A, B, C, D, E\}$

The set of values $E^{(2)}_{\alpha\beta}$ introduced in eqn. (14) corresponds to the energies calculated

by means of eqn. (13). Using n_α we can define

$$\langle \mu_Z \rangle = \sum_\alpha \frac{(\mu_Z)_\alpha}{a_\alpha} n_\alpha \tag{15}$$

$$\langle l_Z \rangle = \sum_\alpha l_\alpha n_\alpha \tag{16}$$

$$\langle a \rangle = \sum_\alpha a_\alpha n_\alpha \tag{17}$$

which are, respectively, the average vertical component of the dipole moment, the average thickness of the monolayer when l_α is the thickness along axis Z of the molecule in orientation α, and the average partial molar surface.

RESULTS AND DISCUSSION

The organizations of clusters composed of 11 molecules belonging to the same class of orientation are visualized in Fig. 4. The drawings were obtained from a computer program run according to method 1. The projections with respect to different perspectives are shown. For orientation C and for orientation A, which is, in this case, equivalent to orientation E, no significant ordered molecular arrangements can be observed. For the other orientation, the molecules seem more or less regularly arranged with respect to one another.

In orientation D, the cluster configuration shows that some molecular pairs stand with their methyl groups in inversion with respect to one another. In orientation B, one observes several doublets with their C=O bond projection at 90°. Furthermore, in position C, the plane of the hetero-ring forms an angle of about 8° with the surface plane.

In Table 3 we have recorded the dipole moment projection $(\mu_Z)_\alpha$, the thickness (l_α) and the partial molar area a_α corresponding to the lowest value of conformational energy $(E_{(\alpha)}^{(N)})_{min}$ computed following method 1.

The areas a_α indicate that orientation B forms the most compact molecular arrangement (of about 5×10^{18} molecules m^{-2}). It is noteworthy that these partial molecular areas are larger than usually considered for the case of adsorbed solvent monolayers [10,11,13]. However, these values are consistent with the magnitude of

TABLE 3

	A	B	C	D	E
$(\mu_Z)_\alpha$/D	−4.85	−3.7	−0.9	−4.1	+4.85
l_α/nm	0.48	0.38	0.22	0.37	0.61
a_α/nm^2	0.289	0.197	0.288	0.242	0.289
$E_{(\alpha)}^{(N)\mathrm{Im}}$/kJ mol^{-1}	−9.0	−9.0	−10.0	−1.0	−7.0
$E_{(\alpha)}^{(N)\mathrm{M.L.}}$/kJ mol^{-1}	−11.0	−11.0	−34.0	−18.0	−9.5

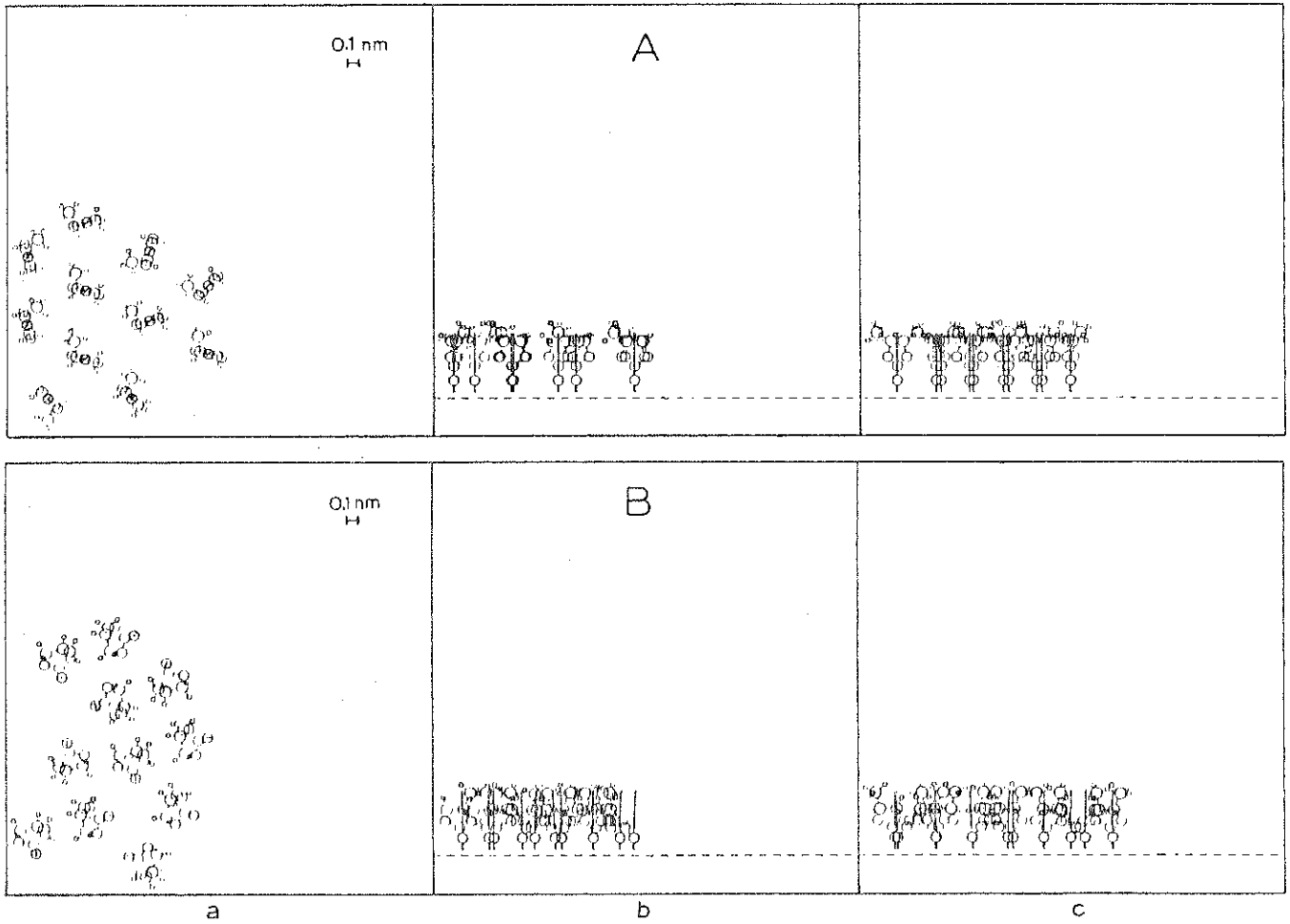
0.1 nm
H
A
0.1 nm
H
B
a
b
c

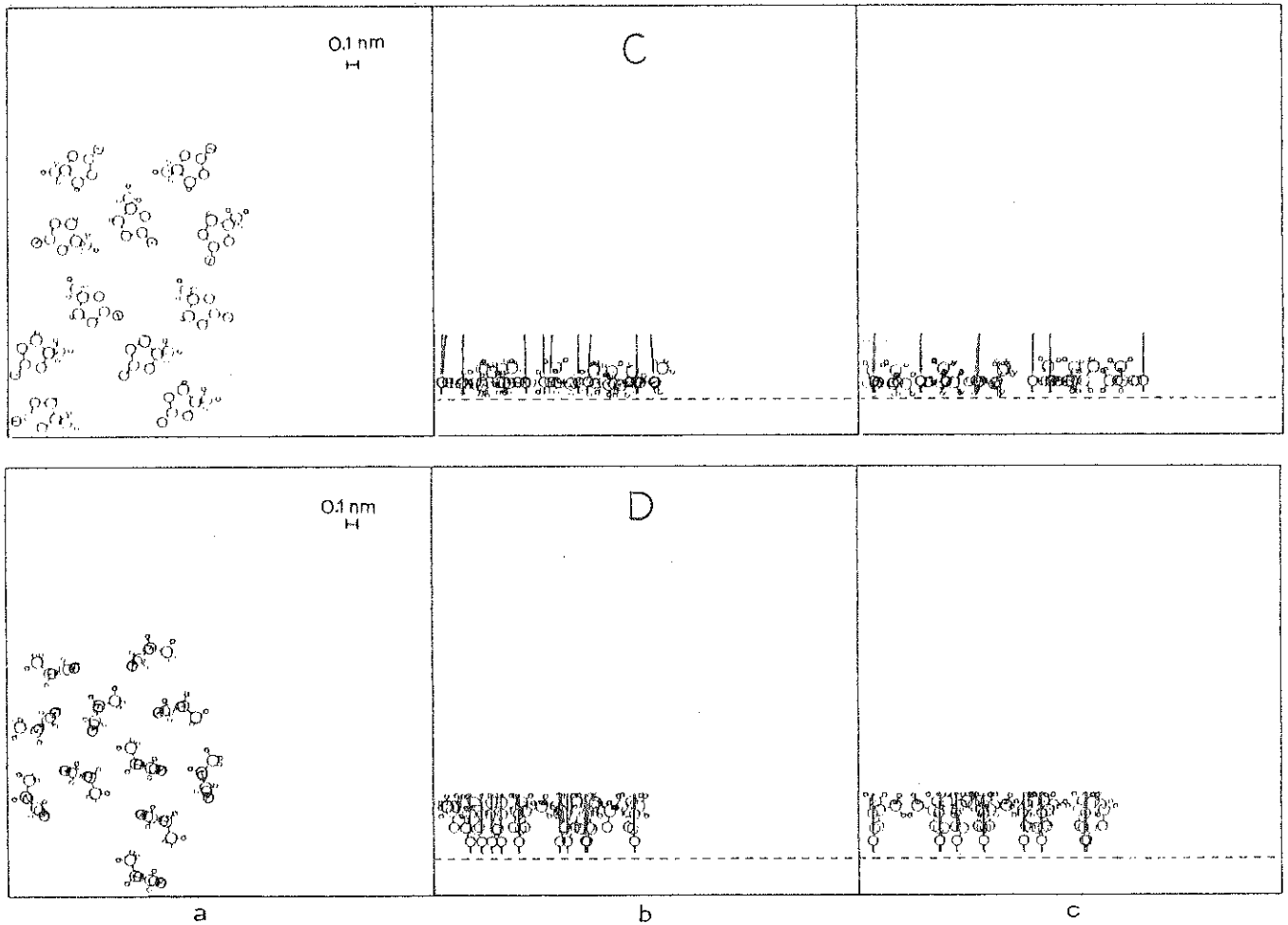

Fig. 4. Schematic presentation of arrangement of molecules at the surface from a program run on method 1: (a) perspective from above the surface (solution side); (b) perspective down side of (a); (c) perspective from the left–right side of (a).

the intermolecular distances calculated on the basis of the sum of the van der Waals radii of two atoms or atomic groups belonging to two different PC molecules.

Application of method 2 gives the change of stability of pairs as a function of the intermolecular distance. It shows that, at surface concentrations $> 5 \times 10^{18}$ molecules m^{-2}, molecules in position B form the most stable pairs in a manner as displayed in Fig. 5. Indeed one observes that such an arrangement furnishes the shortest approach distance between atoms with given point charges of the first molecule and atoms with opposite point charges of the second molecule.

The pairwise energies $E_{(\alpha)}^{(N)}$ have been computed according to strategy 3 at 25°C. In the first case this has been done in the absence of Debye and London types of van der Waals interaction with the metal (the $E_{(\alpha)}^{(N)\mathrm{M.L.}}$ and $E_{(\alpha)}^{(N)\mathrm{Im}}$ energy terms). The value of ϵ_r has been chosen equal to 9. These energies are plotted in Fig. 6a as a function of q. Near the pzc. one observes that the most stable pairs take the orientations CB and CD. With large electric fields, however, the occurrence of orientation C is less probable; this is because of its small vertical dipole moment. With large positive charges, orientations A, D and B play a role whose importance increases according to the sequence of the values of their dipole moments μ_Z. With negative charges, orientation E is dominant and the pairs E–E are most stable, despite the point-dipole–point-dipole repulsion. In the other case, the total pairwise energies $E_{(\alpha)}^{(N)}$, which include all the interaction terms taken up in eqn. (11), are shown in Fig. 6b. As a result of the strong interaction between the Hg phase and the PC molecule in orientation C, groupings C–C are prevalent over nearly all the experimental domain. With large external electric fields, molecules in orientation C remain present, forming pairs with molecules either in orientation B and D on the anodic side or in orientation E on the cathodic side. Because of unfavourable van der Waals interactions between molecules respectively in orientations A, B or C, the occurrence of orientation A is detectable only at the most extreme positive side.

These properties of $E_{(\alpha)}^{(N)}$ are reflected in the values of the distribution function n_α which are recorded in Fig. 7. One can infer from these results that position C prevails with a proportion > 50% over all the experimental domain and reaches a

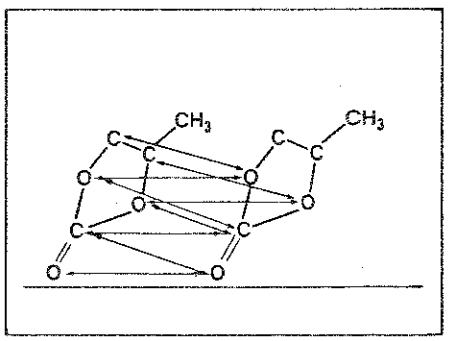

Fig. 5. Most stable configuration of molecular pairs in orientation B at small intermolecular distances.

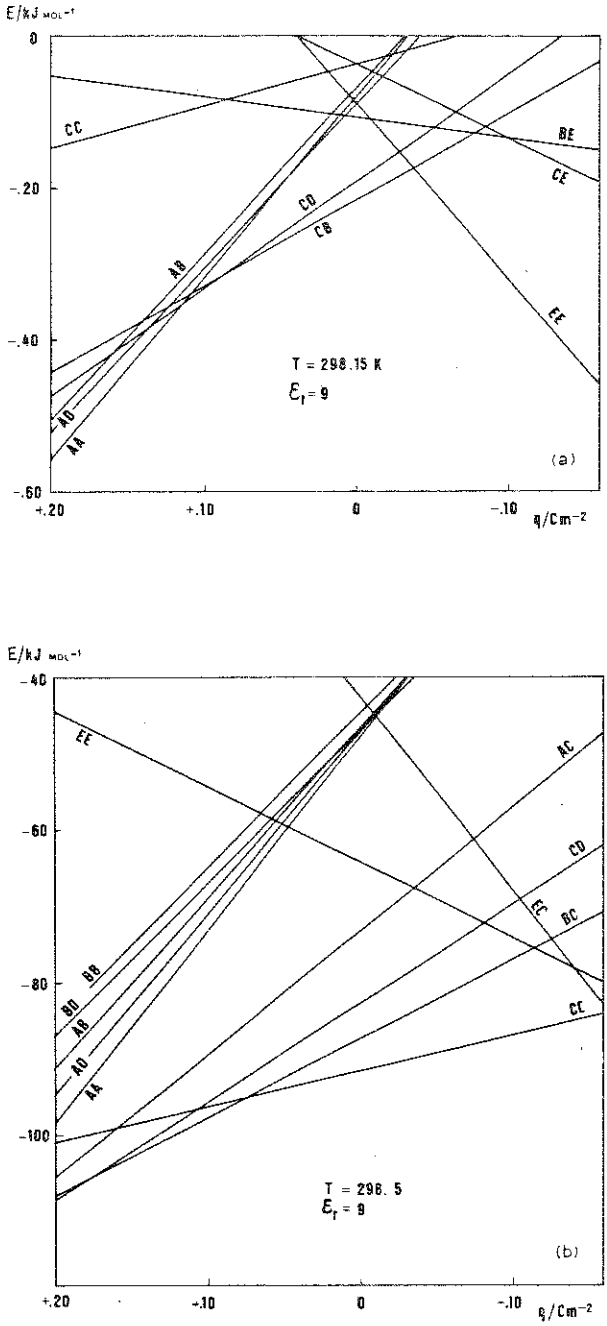

Fig. 6. Conformational energies of pairs at the mercury electrode as a function of charge densities: (a) without, and (b) including $E_{(\alpha)}^{(N)ML}$ and $E_{(\alpha)}^{(N)Im}$ energy terms.

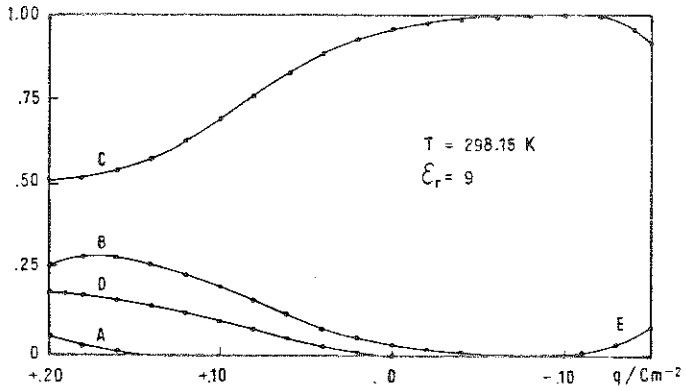

Fig. 7. The distribution function vs. charge densities for different molecular orientations at the surface.

maximum of 99% at about -8×10^{-2} C m^{-2}. The up (E) and down (A) orientations can only be detected at the most positive and negative fields. The average dipole moment component $\langle \mu_Z \rangle$, its differential with respect to q and the average thickness $\langle l_Z \rangle$ at 25°C have been computed by means of n_α. These quantities are shown in Fig. 8. The average potential drop across the monolayer can be derived approximatively from the relation

$$\Delta\phi = \langle l_Z \rangle \frac{q}{\varepsilon_0} - \frac{\langle \alpha \rangle}{\langle a \rangle}\left(\frac{q}{\varepsilon_0} + \chi_{pol}\right) + \frac{\langle \mu_Z \rangle}{\varepsilon_0} \tag{12}$$

where the second term on the rhs represents the contribution of the induced dipole moments of molecules whose mean polarizabilities are denoted by $\langle \alpha \rangle$. According to eqns. (9), (10) and (12), we have the following formula for the reciprocal of the differential inner-layer capacitance C_i:

$$\frac{1}{C_i} = 113.1\left[\frac{\langle l_Z \rangle}{\varepsilon_r}\left(\varepsilon_r - \frac{\langle \alpha \rangle}{\langle a \rangle \langle l_Z \rangle}\right) + \frac{10^{-2}}{3}\frac{\mathrm{d}\langle \mu_Z \rangle}{\mathrm{d}q}\right] (\mathrm{m^2\ F^{-1}}) \tag{13}$$

with $\langle l_Z \rangle$, $\langle a \rangle$ and $\langle \alpha \rangle$ expressed respectively in nm, nm^2 and nm^3: q in C m^{-2} and $\langle \mu_Z \rangle$ in D nm^{-2}. Although the statistical mechanical calculation developed above, on the basis of doublets, represents only a crude attempt at describing equilibrium properties in the monolayer, we have constructed, by means of eqn. (13), a theoretical C_i curve. The calculations performed with $\varepsilon_r = 9$, $\langle \alpha \rangle = 0.090$ nm^3 at 25°C are given in Fig. 9 and compared to the experimental results [6]. On the theoretical curve we have indicated the major effects with respect to the modification of the orientation of small amounts of molecules. Position C predominates in the shallow cathodic part. Increasing proportions of orientations B and D on the anodic side and E on the cathodic side determine the rise on each side of the capacitance. The increase of C_i at large positive charge results essentially from the substitution of orientation B by A. As such, the shape of the capacitance hump seems to be caused

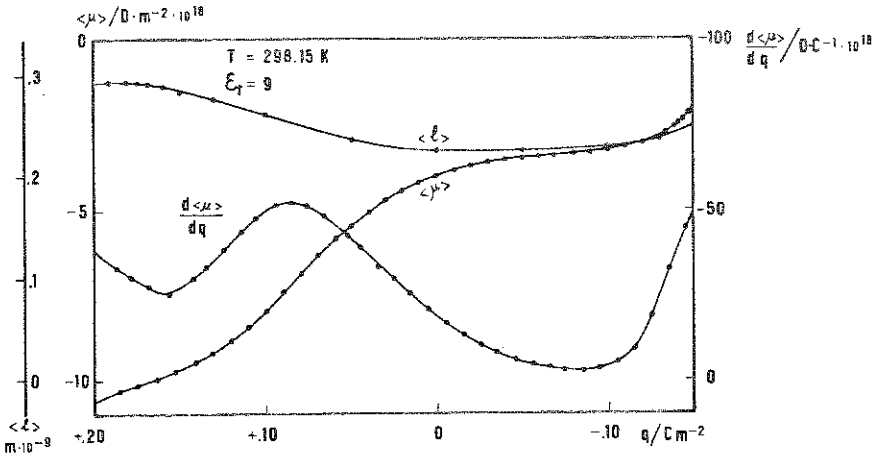

Fig. 8. The average molecular thickness $\langle l_z \rangle$, the average vertical component of the molecular dipole $\langle \mu_z \rangle$ and its derivative with respect to the charge density $d\langle \mu_z \rangle / dq$.

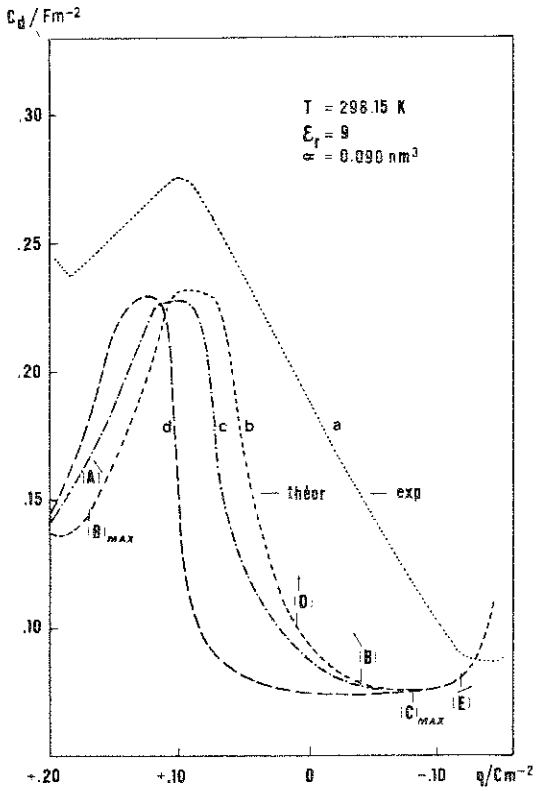

Fig. 9. Differential capacity of the monomolecular layer as a function of charge density: (a) experimental curve; (b) theoretical curve with orientations A, B, C, D, E; (c) theoretical curve without orientation D; (d) theoretical curve without orientation B.

by the re-erecting process following the orientation sequence $C \rightarrow B \simeq D \rightarrow A$ of approximatively 50% of molecules as a maximum. The absence of orientation B in this process acts more dramatically on the shape of C_i than the absence of D. This is illustrated by curves (c) and (d) in Fig. 9 which have been obtained from calculations performed respectively without orientation D and orientation B. In a model limited to orientations A, C, D and E, the curve rise happens to be much faster. Conversely, one would expect that a more continuous sequence of positions between C and A like that given by a multistate model, would lead to a slower rise of C_i beginning at more negative charges. Accordingly, this would yield a better agreement with the experimental results.

The influence of temperature upon the theoretical values of C_i is reported in Fig. 10. The crossing-points at positive and negative charges, at which C_i becomes independent of T are found experimentally at about $+17 \times 10^{-2}$ and -6×10^{-2} C m^{-2} [6]. These crossing-points are observed for a reason that cannot adequately be explained in molecular terms [25]. In the case of water, these points have also been found by using a point-dipole model [11,26]. All we know for certain is the following

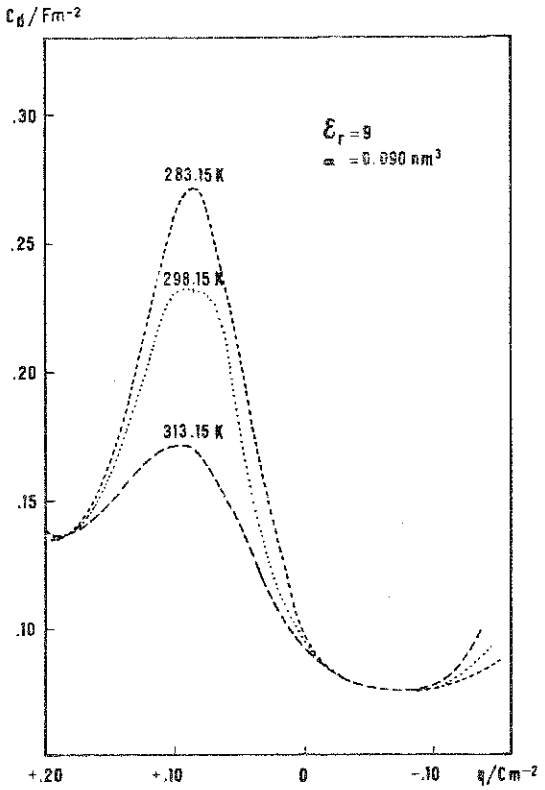

Fig. 10. Theoretical differential capacity as a function of charge density at different temperatures.

relationship between the surface phase entropy S^σ of the monolayer and C_i [6]:

$$\left(\frac{\partial}{\partial T}\frac{1}{C_i}\right)_q = \left(\frac{\partial^2 S^\sigma}{\partial q^2}\right)_T = 0 \tag{14}$$

which provides us with the thermodynamic condition for these crossing-points. Let us emphasize, however, that, except for these two points, the theoretical values disagree with the experimental ones because the former do not give the maximum entropy which is observed at about -0.05 C m^{-2} [6].

As stressed earlier, the above treatment uses two adjustable parameters ε_r and $\langle\alpha\rangle$. If, for example, $\varepsilon_r = 8$ or $\varepsilon_r = 11$ were selected, the maximums of C_i were respectively equal to 0.32 and 0.11 C m^{-2}. The slope of C_i is also rather sensitive to the magnitude of $\langle\alpha\rangle$. The value of $\alpha = 0.09$ nm^3 which has been retained for the best fit with the experimental results is somewhat smaller than the value used by Fawcett [10] in the three-state model for ethylene carbonate, but considerably larger than the experimental mean value of 6.7×10^{-3} nm^3 calculated from the refractive index of this molecule [27]. Fawcett [10] considers that this experimental value is certainly too low since it accounts only for the electronic polarizabilities and ignores the atomic polarizabilities.

Furthermore, hyperpolarizability terms [28] might contribute to the considerable increase of the value of $\langle\alpha\rangle$ because of the very high value of the net electric field experienced by the solvent monolayer. This can be estimated from the potential drop across the monolayer which is 1.2 V at the pzc. This is about twice the value obtained in the three-state model for ethylene carbonate (0.49 V) where a somewhat larger value of $\langle\alpha\rangle$ was assumed (0.11 nm^3) [10], and it is half the value obtained on the basis of the two-state model (2.30 V) [2].

CONCLUSION

Our treatment illustrates, in a preliminary way, how a conformational analysis, based upon a semi-empirical description of intermolecular forces might contribute to an understanding of adsorption phenomena of neutral molecules at the metal surface. The strongest limitations of our model are a result of the following approximations:

(1) a limited number of molecular orientations;

(2) a choice of arbitrary parameters used in handling the molecular polarizability;

(3) a monolayer with discontinuous boundaries;

(4) doublet interactions representing the intermolecular energy terms in the distribution functions.

Presently, improvements in the calculation of the distribution functions are in progress in which we consider energy terms corresponding to larger molecular clusters.

ACKNOWLEDGEMENT

One of the authors (H.D.H.) gratefully acknowledges the financial assistance of NATO.

APPENDIX

Applying the rule of geometrical mean of the interaction parameters, we express the potential energy of interaction between an individual atom i of an adsorbed molecule and an atom of Hg in the metal phase as follows:

$$\varepsilon_{i,\mathrm{Hg}} = -\beta/r_{i,\mathrm{Hg}}^6 = -\sqrt{\beta_{\mathrm{HgHg}}\beta_{ii}}/r_{i,\mathrm{Hg}}^6 \tag{A1}$$

where β_{HgHg} and β_{ii} represent respectively the London interaction parameters for metal-phase Hg atoms and for i atoms and $r_{i,\mathrm{Hg}}$ is the distance separating both atoms. In Fig. A1, the i atom is located at distance Z_i from the metal surface. We picture the metal phase as being composed of smeared-out atoms in sheets which run parallel to the surface.

Under these conditions, each atom i interacts with an infinite stack of these sheets. Those are of thickness δ, of uniform density ρ' and are separated by distance d. The centre of the first sheet is at a distance from the geometrical surface equal to the van der Waals radius of Hg, r_{Hg}. The total potential energy between an atom i and the atoms belonging to an infinite stack of sheets of infinite extension is given by

$$E_i^{\mathrm{M.L.}} = -\sum_{n=0}^{\infty} \frac{\rho'\delta N_{\mathrm{Av}}}{M}\beta\int_0^{\infty} \frac{2\pi Y_i \mathrm{d}Y_i}{\left[\left(\xi_i + n(d+\delta)\right)^2 + Y_i^2\right]^3} \tag{A2}$$

where $\xi_i = Z_i + r_{\mathrm{Hg}}$.

The condition that the amount of Hg is conserved allows us to express the average uniform density ρ of the metal phase as

$$\rho = \rho'\delta/(d+\delta) \tag{A3}$$

Furthermore, the Hamaker constant of Hg is defined as

$$A_{\mathrm{Hg}} = \left(\rho N_{\mathrm{Av}}\pi^2/M\right)\beta_{\mathrm{HgHg}} \tag{A4}$$

Incorporating the alternative way of deriving A_{Hg} from the dispersion component of the surface tension of Hg, $\gamma_{\mathrm{Hg}}^{\mathrm{d}}$, as suggested by Fowkes, (24) we obtain

$$A_{\mathrm{Hg}} = (4\pi/1.2)d^2\,\gamma_{\mathrm{Hg}}^{\mathrm{d}} \tag{A5}$$

where $\gamma_{\mathrm{Hg}}^{\mathrm{d}} = 200\ \mathrm{mN\ m^{-1}}$.

Using eqns. (A1) and (A3)–(A5) and taking the limit $\delta \to 0$, we integrate eqn. (A2). Then the potential energy becomes

$$E_i^{\mathrm{M.L.}} = -H_{i,\mathrm{Hg}}\sum_{n=0}^{\infty}\left(\xi + nd\right)^{-4} \tag{A6}$$

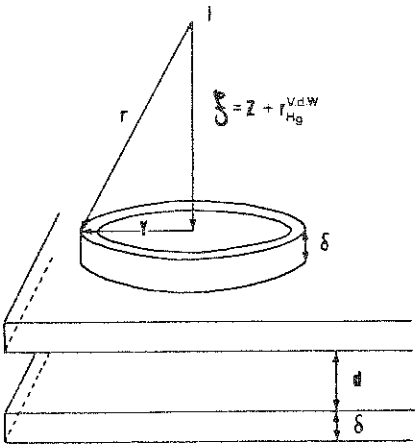

Fig. A1. The model for the computation of atom–metal phase dispersive interaction energies.

where

$$H_{i,Hg} = \sqrt{\gamma_{Hg}^{d}(M/1.2)\beta_{ii}d^4} \tag{A7}$$

Application of eqn. (A6) reveals that most frequently more than 80% of the total potential energy arises from the interaction between an atom i and the first sheet of Hg atoms.

REFERENCES

1 T. Biegler and R. Parsons, J. Electroanal. Chem., 21 (1969) App. 4.
2 W.R. Fawcett and M.D. Mackey, J. Chem. Soc. Faraday Trans. I, 69 (1973) 634.
3 R. Payne, J. Am. Chem. Soc., 89 (1967) 489.
4 J. Lawrence and R. Parsons, Trans. Faraday Soc., 64 (1968) 751.
5 W.R. Fawcett and R.O. Loutfy, Can. J. Chem., 51 (1973) 230.
6 N.H. Cuong, A. Jenard and H.D. Hurwitz, J. Electroanal. Chem., 103 (1979) 344.
7 R.J. Watts-Tobin, Phil. Mag., 6 (1961) 133.
8 N.F. Mott and R.J. Watts-Tobin, Electrochim. Acta, 4 (1961) 79.
9 R. Payne, Adv. Electrochem. Electrochem. Eng., 7 (1970) 1.
10 W.R. Fawcett, J. Phys. Chem., 82 (1978) 1385.
11 W.R. Fawcett, Isr. J. Chem., 18 (1979) 3.
12 Z. Borkowska, R.M. de Nobriga and R.W. Fawcett, J. Electroanal. Chem., 124 (1981) 263.
13 W.R. Fawcett and R.M. de Nobriga, J. Phys. Chem., 86 (1982) 371.
14 E. Ralston and J.L. De Coen, J. Mol. Biol., 83 (1974) 393.
15 J.L. De Coen, G. Elefante, A.M. Liquori and A. Damiani, Nature 216 (1967) 910.
16 A.M. Liquori, E. Giglio and L. Mazzarella, Nuovo Cimento, 55B (1968) 475.
17 E. Giglio, A.M. Liquori and L. Mazzarella, Nuovo Cimento, 56B (1968) 57.
18 R. Scordamaglia, F. Cavallone and E. Clementi, J. Am. Chem. Soc., 99 (1977) 5545.
19 E. Giglio, Nature, 222 (1969) 339.
20 A.M. Liquori, Q. Rev. Biophys., 2 (1969) 65.

21 J.L. De Coen and E. Ralston, Biopolymers, 16 (1971) 1929.
22 H.L. Yeager, J.D. Fedyk and R.J. Parker, J. Phys. Chem., 77 (1973) 2407.
23 T.N. Andersen and J.O'M. Bockris, Electrochim. Acta, 9 (1964) 347.
24 F.M. Fowkes, Ind. Eng. Chem., 56 (1964) 40.
25 Z. Borkowska, W.R. Fawcett and S. Anantawan, J. Phys. Chem., 84 (1980) 2769.
26 R. Parsons, J. Electroanal. Chem., 59 (1975) 229.
27 R. Kempa and W.H. Lee, J. Chem. Soc., (1958) 1936.
28 A.D. Buckingham and B.J. Orr, Q. Rev. Chem. Soc., 21 (1967) 195.